MOLECULAR CARCINOGENESIS 45:461–478 (2006)

Checkpoint Kinase 1-Mediated Phosphorylation of Cdc25C and Bad Proteins Are Involved in Antitumor Effects of Loratadine-Induced G_2/M Phase Cell-Cycle Arrest and Apoptosis

Jinn-Shiun Chen,[1] Shyr-Yi Lin,[2] Wei-Ling Tso,[3] Geng-Chang Yeh,[4] Wen-Sen Lee,[5] How Tseng,[6] Li-Ching Chen,[7] and Yuan-Soon Ho[3]*

[1]*Division of Colon and Rectal Surgery, Department of Surgery, Chang Gung Memorial Hospital, Linkou, Taiwan*
[2]*Department of Internal Medicine, School of Medicine, Taipei Medical University, Taipei, Taiwan*
[3]*Graduate Institute of Biomedical Technology, Taipei Medical University, Taipei, Taiwan*
[4]*Graduate Institute of Medical Sciences, and Department of Pediatrics, School of Medicine, Taipei Medical University, Taipei, Taiwan*
[5]*Graduate Institute of Medical Sciences, and Department of Physiology, School of Medicine, Taipei Medical University, Taipei, Taiwan*
[6]*Graduate Institute of Medical Sciences, School of Medicine, Taipei Medical University, Taipei, Taiwan*
[7]*Institute of Biomedical Sciences, Academia Sinica, Taipei, Taiwan*

In this study, we first demonstrated that loratadine (LOR), a promising world widely used oral anti-histamine, effectively inhibits growth of tumors derived from human colon cancer cells (COLO 205) in an in vivo setting. In vitro study demonstrated that the anti-tumor effects of LOR in COLO 205 cells were mediated by causing G_2/M phase cell growth cycle arrest and caspase 9-mediated apoptosis. Cell-cycle arrest induced by LOR (75 μM, 24 h) was associated with a significant decrease in protein levels of cyclin B1, cell division cycle (Cdc) 25B, and Cdc25C, leading to accumulation of Tyr-15-phosphorylated Cdc2 (inactive form). Interestingly, LOR (75 μM, for 4 h) treatment also resulted in a rapid and sustained phosphorylation of Cdc25C at Ser-216, leading to its translocation from the nucleus to the cytoplasm because of increased binding with 14-3-3. We further demonstrated that the LOR-induced Cdc25C (Ser-216) phosphorylation was blocked in the presence of checkpoint kinase 1 (Chk1) specific inhibitor (SB-218078). The cells treated with LOR in the presence of Chk1 specific inhibitor (SB-218078) were then released from G_2/M arrest into apoptosis. These results implied that Chk1-mediated phosphorylation of Cdc25C plays a major role in response to LOR-mediated G_2/M arrest. Although the Chk1-mediated cell growth arrest in response to DNA damage is well documented, our results presented in this study was the first report to describe the Chk1-mediated G_2/M cell-cycle arrest by the histamine H1 antagonist, LOR.

Key words: loratadine; G_2/M arrest; apoptosis; anti-tumor; Chk1

INTRODUCTION

The cell cycle is controlled by the periodic regulation of the highly conserved cyclin dependent kinases (CDKs) [1]. In eukaryotes, the G_2/M checkpoint is controlled by the cell-division cycle (Cdc) 2/Cyclin B complex, whose activity is required for entry into mitosis [2]. Previous studies indicate that Cdc2 (Tyr-15) phosphorylation is maintained during cancer therapeutic drug-induced G_2/M arrest in mammalian cells [3–5]. Phosphorylation of Cdc2 (Tyr-15) is accomplished by two major regulators including Wee1, which phosphorylate Cdc2 at Tyr-15 and Myt1, which phosphorylate Cdc2 at Thr-14 and, to a lesser extent, Tyr-15 [6]. The Cdc2 (Tyr-15) was activated by Cdc25C, a dual specific phosphatase, whose activity is essential for entry into mitosis [7]. In addition, two additional regulators include 14-3-3, which binds Cdc25C and inhibits the import of Cdc25C from ctyoplasm into the nucleus, and checkpoint kinase 1 (Chk1), which phosphorylate Cdc25C at Ser-216 and creates a consensus-binding site for 14-3-3 [8]. The binding of 14-3-3 requires the

Abbreviations: Cdc 25B, cell-division cycle 25B; Chk1, checkpoint kinase 1; LOR, loratadine; ATR, ataxia telangiectasia-mutated and Rad 3-related; FCS, Fetal calf serum; DBH, debromohymenialdisine; DMSO, dimethylsulfoxide; PBS, phosphate-buffered saline; P.I., propidium iodide; FACS, fluorescence activated cell sorting; pNA, *p*-nitroaniline; CCCP, carbonyl cyanide *m*-chlorophenylhydrazone; Val, valinomycin; I.P., intraperitoneal; TF, terfenadine; ATM, ataxia telangiectasia-mutated.

*Correspondence to: Graduate Institute of Biomedical Technology, Taipei Medical University, 250 Wu-Hsing Street, Taipei 110, Taiwan.

Received 20 June 2005; Revised 22 September 2005; Accepted 11 October 2005

DOI 10.1002/mc.20165

phosphorylation of Cdc25C at Ser-216, and mutating this residue to Ala abolishes the interaction [9]. This site is present in the potential recognition motif for 14-3-3 and is phosphorylated in vitro by checkpoint kinases, such as Chk1 and Chk2 [10,11]. These results leads to the nuclear export of Cdc25C and its subsequent cytoplasmic sequestration by 14-3-3 protein, which prevents the activation of the downstream target of Cdc25C, the cyclin B/Cdc2 kinase that is responsible for G_2/M transition. Thus, the association of 14-3-3 with target proteins could modulate cell-cycle progression through different mechanisms such as subcellular localization and enzyme activity, depending on cellular signaling.

It has been well demonstrated that Chk1 inhibition potentiate the cytotoxicity of DNA-damaging drugs through abrogation of the cell-cycle checkpoint [12–14]. However, several agents that including anti-mitotic agent (paclitaxel) [15], topoisomerase II inhibitor (etoposide, camptothecin, and doxorubicin) [12,16], and microtubule-targeting agents (nocodazole) [17] which were not targeted on DNA damage also revealed that G_2/M arrest is largely dependent on Chk1-mediated signaling pathway. In this study, the Chk1 was demonstrated to play some important role in the loratadine (LOR)-induced mitotic checkpoint. Our study also implied that the clinical efficacy of anti-tumorigenesis was expected to be enhanced by Chk1 inhibitor, as evidenced by released of the G_2/M phase arrest cells into apoptosis.

In the present study, we demonstrate that LOR treatment causes a G_2/M phase cell-cycle arrest in COLO 205 cells which is associated with a marked decrease in the expression of key G_2/M-regulating proteins, including cyclin B1, Cdc25B, and Cdc25C. In addition, we provide evidence to indicate that cell-cycle arrest in LOR-treated COLO 205 cells is caused by ataxia-telangiectasia-mutated and Rad3-related (ATR) /Chk1-mediated phosphorylation of Cdc25C at Ser-216. Phosphorylation of Cdc25C in LOR-treated cells leads to its sequestration in the cytosol through increased binding with 14-3-3. Recent studies demonstrated that ATR/Chk1 is postulated in response to DNA damage by ionizing radiation, UV light, or interference with DNA replication [18–20]. In this study, our results provide further evidence showing that Chk1 signaling regulatory proteins may be predominantly affect the LOR-mediated G_2/M cell-cycle checkpoint response.

MATERIALS AND METHODS

Chemicals and Reagents

Protease inhibitors (phenylmethyl sulfonyl fluoride (PMSF), pepstatin A, leupeptin, and aprotinin) were acquired from Sigma Chemical Company (Sigma Aldrich Chemie GmbH, Steinheim, Germany). Dulbecco's modified Eagle's medium (DMEM), Fetal calf serum (FCS), penicillin/streptomycin solution, and fungizone were purchased from Gibco-Life Technologies (Paisley, UK). The chemical inhibitors were obtained from various sources as indicated: The Chk1 inhibitors SB-218078 [21], and the Chk1/Chk2 inhibitor debromohymenialdisine (DBH) [22,23] were from Calbiochem (San Diego, CA).

Antibodies

The following monoclonal antibodies were obtained from various sources as indicated: anti-caspase-8, anti-cytochrome C, anti-cyclin B1, anti-Chk1 (sc-8408 or sc-7898), anti-Chk2 (sc-5278), anti-Cdc25B, anti-GAPDH, anti-AIF, and anti-14-3-3 antibodies (Santa Cruz Biotechnology, Santa Cruz, CA), anti-phosphor BAD (Ser-155) (Cell Signaling Technology, Beverly, MA), anti-PCNA (Dako Corporation, Denmark), anti-caspase 9, anti-caspase 3 antibodies (Stressgen Biotechnologies, Victoria, BC, Canada), anti-cytochrome C oxidase, (Research Diagnostics, Flanders, NJ), and anti-β-actin (Sigma Aldrich Chemie GmbH). The rabbit polyclonal antibodies against phospho-Chk1 (Ser-345), phospho-Chk2 (Thr-68), phospho-Cdc2 (Tyr-15), Cdc2, phospho-Cdc25C (Ser-216), and Cdc25C (C-20) were purchased from Cell Signaling Technology.

Cells and Culture Conditions

The COLO 205 cell line was isolated from human colon adenocarcinoma (American Type Culture Collection CCL-222). The cell line FCH, a homozygous familial hypercholesterolemia cell (CRL 1831; American Type Culture Collection), was derived from primary cultures of normal CRLs [24]. The cells were grown in RPMI 1640 supplemented with 10% FCS, penicillin (100 U/ml), streptomycin (100 mg/ml), and 0.3 mg/ml of glutamine for COLO 205; grown in DMEM/Ham's Nutrient Mixture F-12, 1:1 with 2.5 mM L-glutamine, 1.2 g/L sodium bicarbonate, 15 mM HEPES and 0.5 mM sodium pyruvate supplemented with 10% FCS, 10 ng/ml of cholera toxin, 0.005 mg/ml of insulin, 0.005 mg/ml of transferrin, 100 ng/ml of hydrocortisone, and 10 mM HEPES for CRL 1831 in a humidified incubator (37°C, 5% CO_2). LOR (Sigma Chemical Co., St. Louis, MO) was added at the indicated doses in 0.05% dimethylsulfoxide (DMSO). For control treated cells, the same volume of DMSO was added in a final concentration of 0.05% (v/v) without LOR.

Determination of Cell Viability

COLO 205 and CRL 1831 cells were treated with LOR (10–75 μM). Cell viability was determined at the indicated times based on 3-(4,5-dimethylthiazol-2-yl)-2,5-diphenyl-^{2}H-tetrazolium bromide (MTT) assay. Briefly, cells were seeded in a 96-well plate at a density of 1×10^4 cells/well and allowed to adhere overnight. After removing the medium, 200 μl of

fresh medium per well, containing 10 mmol/L HEPES (pH 7.4) was then added. Then, 50 μl of MTT was added to the wells and the plate was incubated for 2–4 h at 37°C in the dark. The medium was removed and 200 μl DMSO and 25 μl Sorensens's glycine buffer was added to the wells. Absorbance was measured using an ELISA plate reader at 570 nm.

Cell synchronization, drug treatment, and flowcytometric analysis

At 24 h after plating of cells, cells were washed twice with phosphate-buffered saline (PBS) and then incubated with medium containing 0.04% FCS for additional 24 h. Under such conditions, cells were arrested in G_0/G_1 as determined by using flowcytometric analysis [25]. After serum starvation, the low-serum (0.04% FCS) medium was removed and the cells were then challenged by addition of medium containing 10% FCS. LOR solutions were prepared in a final concentration of 0.05% (v/v) DMSO. The cell-cycle stages in the LOR and DMSO-treated groups were measured by flowcytometric analysis. Cells were harvested and stained with propidium iodide (P.I.) (50 μg/ml) (Sigma Chemical Co.), and DNA content was measured using a fluorescence activated cell sorting (FACS) can laser flowcytometry analysis system (Becton–Dickinson, San Jose, CA); and 15000 events were analyzed for each sample.

Western Blotting Analysis

Western blotting analysis was performed as described previously [26]. Briefly, cell lysates were prepared, electrotransferred, immunoblotted with antibodies, and then visualized by incubating with the colorigenic substrates (nitroblue tetrazolium, NBT and 5-bromo-4-chloro-3-indolyl phosphate (BCIP)) (Sigma Chemical Co.). The expression of either GAPDH, β-actin, or cytochrome C oxidase was used as control for equal protein loading.

Immunoprecipitation

Equal amounts of protein were immunoprecipitated with saturating amounts of anti-14-3-3 antibody. Immunoprecipitates were washed five times with extraction buffer and once with PBS. The pellet was then resuspended in sample buffer (50 mM Tris, pH 6.8; 100 mM dithiothreitol; 2% SDS; 0.1% bromophenol blue; 10% glycerol) and incubated for 10 min at 90°C before electrophoresis to release the proteins from the beads. The 14-3-3-immunoprecipitated phosphor Cdc25C and phosphor BAD proteins were then measured by Western blot analysis using specific antibodies.

Isolation of Mitochondria and Cytosolic Fractions of Cell Lysates [27]

The COLO 205 cells were incubated with LOR (25 μM) for the indicated time points and then assayed for translocation of cytochrome C from the mitochondria membrane into cytosol. Lysis of cells for mitochondrial protein extraction was performed in isotonic buffer (200 mM mannitol, 70 mM sucrose, 1 mM EGTA, 10 mM HEPES, pH 6.9) by dounce homogenization. Unbroken cells, nuclei, and heavy membranes were pelleted at 1000*g* for 5 min and discarded. The mitochondrial enriched fraction was collected by pelleting at 12000*g* for 20 min. The pellet was then washed briefly in alkaline wash buffer (0.1 M Na_2CO_3, pH 11.5) to separate peripherally associated (alkali sensitive) mitochondrial proteins from membrane integrated (alkali resistant) mitochondrial proteins and centrifuged. The pellet (containing the membrane integrated proteins) was resuspensed in RIPA lysis buffer (1× PBS, 1% Nonidet P-40, 0.5% sodium deoxycholate, 0.1% sodium dodecyl sulphate) with protease inhibitor cocktail (Calbiochem) and used for immunoblotting. For cytochrome C oxidase protein detection (cytochrome C oxidase, subunit IV, detection was employed as a control to demonstrate that mitochondrial protein fractionation was successfully isolated), equivalent samples (20 μl containing approximately 50 mg protein) were separated by SDS–PAGE on 12% Tris glycine gels and transferred to 0.2 mM polyvinylidene difluoride membranes (Invitrogen). Blots were probed with a mouse monoclonal antiserum specific for cytochrome C (Santa Cruz, CA) or with a rabbit polyclonal antibody specific for cytochrome C oxidase followed by the appropriate secondary antibodies conjugated to horseradish peroxidase (Santa Cruz) and then visualized by Super-Signal chemiluminescence kit as described in the manufacturer's protocol (Pierce Biotechnology, Rockford, IL) and visualized by autoradiography.

Preparation of Nuclear and Cytoplasmic Fractions

Nuclear and cytoplasmic fractions from control (DMSO-treated) and LOR-treated COLO 205 cells were prepared as described previously [5]. Briefly, cells were harvested by scraping and rinsed twice in ice-cold PBS. The cells were then swollen in ice-cold hypotonic lysis buffer (20 mM HEPES, pH 7.1, 5 mM KCl, 1 mM $MgCl_2$, 10 mM *N*-ethylmaleimide, 0.5 mM phenylmethylsulfonyl fluoride, 5 μg/ml of pepstatin A, 2 μg/ml of chymostatin, 5 μg/ml of leupeptin, 5 μg/ml of aprotinin, 5 μg/ml of anti-pain) for 10 min. The cells were lysed by 20 strokes in a Dounce homogenizer, and the nuclei were cleared by centrifugation (400*g*, 10 min). After this step, the supernatant (cytosolic fraction) was concentrated and stored at −80°C. The nuclear extract was prepared using the same lysis buffer and stored at −80°C prior to Western blot analysis for Cdc25C. The blot was stripped and reprobed with β-actin or PCNA antibody to ensure equal protein loading as well as to rule out cross contamination of cytoplasmic and nuclear fractions.

Chk1 Kinase Activity Assay

Approximately 10^6 cells were plated at a confluence of ~70% and exposed to LOR (75 μM, 4 h). Cells were collected, and Chk1 kinase activity was measured by a immunoprecipitation kinase assay as described previously [28,29]. Briefly, the Chk1 assay was carried out in 50 μl volume in the following buffer: 20 mM Na-HEPES, pH 7.4, 50 mM KCl, 1 mM EGTA, 10 mM $MgCl_2$, and 1 mM DTT. A synthetic peptide with a sequence flanking Ser-216 of human Cdc25C, KVSRSGLYRSPSMPENLNRK, was used as its substrate [29]. Chk1 was used at 5 nM, the peptide was used at 20 μM, and [γ-^{32}P]ATP was used at 10 μM (final concentration). Reactions were incubated at 37°C for 20 min and stopped by adding 5 μl of acetic acid containing 10 mM ATP. Thirty-microliter samples were spotted on 2-cm phosphocellulose filter disks, which were washed four times, 5 min each with 0.5% phosphoric acid and counted by liquid scintillation. The apparent *Km* for ATP in the Chk1 assay was about 120 μM.

Wee1 Kinase Activity Assay

The recombinant Cdc2 protein was purified as a glutathione S transferase fusion protein containing full-length human Cdc2 (Santa Cruz Biotechnology) and then used as a substrate for Wee1 kinase assay. Glutathione S-transferase protein was used as a negative control substrate and was prepared according to the standard procedure suggested by the manufacturer (Pharmacia, Piscataway, NJ). Preparation of cell lysates, immunoblotting, immunoprecipitation were performed as described previously [25] except that cell lysis buffer for immunoprecipitation was 50 mM Tris-HCL, pH 7.5; 1% Triton X-100; 0.5 mM Na_3VO_4; 50 mM sodium fluoride; 5 mM sodium pyrophosphate; 10 mM sodium 2-glycerophosphate; 0.1 mM PMSF; 1 μg/ml of aprotinin; 1 μg/ml of pepstatin; 1 μg/ml of leupeptin; 1 μM microcystin; 1 mM DTT; 1 mM EDTA, and 1 mM EGTA. Kinase assays for Wee1 were performed as described previously [30,31]. The Wee1 kinase assay used 500 μg of cell extract for immunoprecipitating kinase, and 2 μg of relative protein substrate. Kinase reaction was carried out by incubation for 30 min at 30°C and terminated by addition of 30 μl of 6× Laemmli SDS sample buffer [32]. Substrate phosphorylation was analyzed by SDS-polyacrylamide gel electrophoresis and autoradiography.

Cdc2 Kinase Activity Assay

The method for the assay of the Cdc2 kinase was according to our previous report [26]. The protein content in each sample was determined as described above and adjusted to 100 μg/lane. Lysate (in 0.5 ml of extraction buffer) was immunoprecipitated with 5 μg monoclonal anti-cyclin B1 antibody, the immuno-complexes were washed three times with the lysis buffer and once with kinase buffer containing 50 mM Tris-HCl (pH 7.4), 10 mM $MgCl_2$, and 1 mM dithiothreitol. The beads were incubated with 50 μl of kinase reaction mixture containing 50 mM Tris-HCl (pH 7.4), 10 mM $MgCl_2$, 1 mM dithiothreitol, 10 μM ATP, 5 μCi of [γ-32p] ATP, and 0.5 mg/ml of histone H1 for 15 min. The reaction was terminated by the addition of 20 μl of 4× Laemmlis sample buffer and boiling for 5 min. The ^{32}p-phosphorylated histone H1 was separated by 0.1% SDS, 10% polyacrylamide gel, and determined by autoradiography using Kodak X-Omat film.

Analysis of Apoptosis

Apoptosis in the COLO 205 cells subjected to various treatments was determined by using the DNA fragmentation analysis [33]. Briefly, the LOR and DMSO-treated cells were seeded on 100-mm dishes. The DNA was extracted twice with equal volumes of phenol and once with chloroform-isoamyl alcohol (24:1 v:v), precipitated with 0.1 volume of sodium acetate, pH 4.8, and 2.5 volumes of ethanol at −20°C overnight, and finally centrifuged at 13000*g* for 1 h. Genomic DNA was quantitated, and equal amounts of DNA sample in each lane were electrophoresed in a 2% agarose gel. The DNA was visualized by ethidium bromide staining.

Caspase Activity Assay

Caspase activity was measured by using caspases 3 (Promega, Madison, WI) and 9 (Chemicon, Temecula, CA) colorimetric activity assay kits as previous described [34,35]. Briefly, COLO 205 cells were lysed by addition of cell lysis buffer and protein concentration was measured. Caspase activity was assayed at 37°C in 100 μl of assay buffer containing 50 μg (for caspase 3) or 30 μg (for caspase 9) of the indicated colorimetric peptide. Caspase activity was measured by the release of *p*-nitroaniline (pNA) from the labeled substrates Ac-DEVD-pNA and Ac-LEHD-pNA for caspase 3 and 9, respectively, and the free pNA was quantified at 405 nm.

Mitochondrial Transmembrane Potential Assay

To assess the mitochondrial transmembrane potential ($\Delta\Psi$m), COLO 205 cells (1×10^6) were seeded in a six-well plate washed twice with PBS and then loaded with the cationic lipophilic fluorochrome JC-1 (5 μg/ml) for 10 min at 37°C. Cells were washed twice with PBS and submitted to FACS-analysis. The red fluorescence of JC-1 aggregates corresponds to the mitochondrial membrane potential whereas the green fluorescence of JC-1 monomers is indicative for the mitochondrial mass. Active mitochondria with high $\Delta\Psi$m accumulate JC-1 aggregates, which are red, whereas, in the mitochondria with low $\Delta\Psi$m, JC-1 stays in a monomeric, green

form. This renders the red/green ratio, a sensitive indicator of the mitochondrial $\Delta\Psi$m changes. In addition, carbonyl cyanide *m*-chlorophenylhydrazone (CCCP; Calbiochem) or valinomycin (Val, Sigma) were dissolved in 100% acetone and diluted in complete medium; the acetone concentration in the medium did not exceed 1%. Both of the CCCP and Val were added at a final concentration of 200 μM as a positive control, and the fluorescence was assessed for each time point, a red/green fluorescence ratio was then calculated. The mean red fluorescence of drug-treated cells was measured at 0, 2, 4, 6, 8, 10, and 12 h after LOR treatment, and presented as a ratio of the absorbance in 590/535 nm [36].

Immunofluorescence Staining And Confocal Microscopic Observation

For microscopic observations of nuclear/cytoplasmic and nuclear/mitochondria distribution of Cdc25C and AIF, respectively, COLO 205 cells were incubated in 0.05% DMSO (control) or LOR for the indicated time points. COLO 205 cells were immunostained with monoclonal antibodies specific to phosphor Cdc25C (Ser-216) and AIF (Santa Cruz, CA) for 2 h. After washing with PBS/Tween 20 for three times, monoclonal antibodies were visualized with goat-anti-mouse IgG antibody labeled with FITC (green) for 1 h. Propidium iodide at concentration of 100 ng/ml for 5 min was used for nuclear staining. Stained cells were imaged by confocal scanning microscopy (Olympus, Tokyo, Japan) using excitation/emission wavelengths of 458/488 nm and 543/633 nm for FITC and P.I., respectively.

Treatment of COLO 205-Derived Xenografts In Vivo

COLO 205 cells were grown in RPMI 1640 supplemented with 10% FCS as described in our previous studies [25–27]. Cells were harvested through two consecutive trypsinizations, centrifuged at 300*g* for 5 min, washed twice, and resuspended in sterile PBS. Cells (5×10^6) in 0.2 ml were injected subcutaneously between the scapulae of each nude mouse (purchased from National Science Council Animal Center, Taipei, Taiwan). After transplantation, tumor size was measured using calipers and the tumor volume was estimated according to the formula tumor volume (mm^3) $= L \times W^2/2$, where L is the length and W is the width [26]. Once tumors reached a mean size of 200 mm^3, animals received intraperitoneal (I.P.) injections of either 25 μl DMSO or 25 mg/kg LOR three times per wk for 6 wk.

Statistics

Statistical analysis was carried out using analysis of variance (ANOVA)—one way analysis of variance with Student—Newman correction, and the Student's *t*-test. Significance was assumed for values of $P < 0.05$.

RESULTS

To investigate the antiproliferative effects of LOR, human colon cancer cells (COLO 205) and human normal CRL 1831 were treated with different doses (10–50 μM) of LOR for 1–5 days and the cell growth numbers were then determined (Figure 1A). LOR at lower dose (10 μM) suppressed COLO 205 cell proliferation while at higher dose (25 μM) induced cell death (Figure 1A, left). Interestingly, such effect was less profound when normal human colon epithelial cells (CRL 1831) treated with LOR (Figure 1A, right). These results indicated that colon cancer cells were more susceptible to LOR treatment than normal human CRLs.

To further demonstrate whether the cytotoxic effect induced by LOR was due to apoptotic cell death. The LOR-induced apoptotic effect was evaluated by flowcytometric and DNA fragmentation analysis. As shown in the Figure 1B, both of the sub-G_1 and G_2/M phase populations were observed in COLO 205 cells exposed to 20–50 μM of LOR. Interestingly, G_2/M arrest instead of DNA fragmentation was observed in COLO 205 cells, which exposed to higher dose (75 μM) LOR. Our previous report have demonstrated that apoptosis and G_0/G_1 cell-cycle arrest was induced by terfenadine (TF), an histamine H1 receptor antagonist with a mechanisms similar to LOR [37,38]. In order to demonstrate whether the LOR- or TF-induced apoptosis was mediated through the blockage of the specific histamine H1 receptor signaling pathway, four additional histamine H1 blockers including cetirizine, ebastine, epinastine, and fexofenadine [39] were added to COLO 205 cells (75 μM, 24 h) then detected for DNA laddering effect. Our data demonstrated that DNA fragmentation was observed only in the LOR- and TF-treated group (Figure 1D). Such results suggested that the histamine H1 receptor was not the major apoptosis-signaling sensor in response to LOR in the COLO 205 cells.

To address the cell-cycle effects of LOR, the COLO 205 cells were synchronized at the G_0/G_1 phase by 0.04% serum starvation for 24 h [25,26]. After serum starvation, the complete medium containing 10% FCS was then replaced. The cells treated either with mock-treated (DMSO) or LOR (75 μM) were then measured for cell cycle by flowcytometric analysis. As shown in Figure 2A (right), G_2/M cell-cycle arrest was observed initially at 9 h and reached the maximal level of more than 40% at 24 h after LOR treatment.

It is well established that onset of mitosis is triggered by activation of the Cyclin B1/Cdc2 kinase, which is absolutely required for transition of G_2 cells into M phase [19,40]. During the G_2 phase, Cyclin B1/Cdc2 is inactivated by phosphorylation at the Thr-14 and Tyr-15 residues, which are dephosphorylated by Cdc25C phosphatase before going into

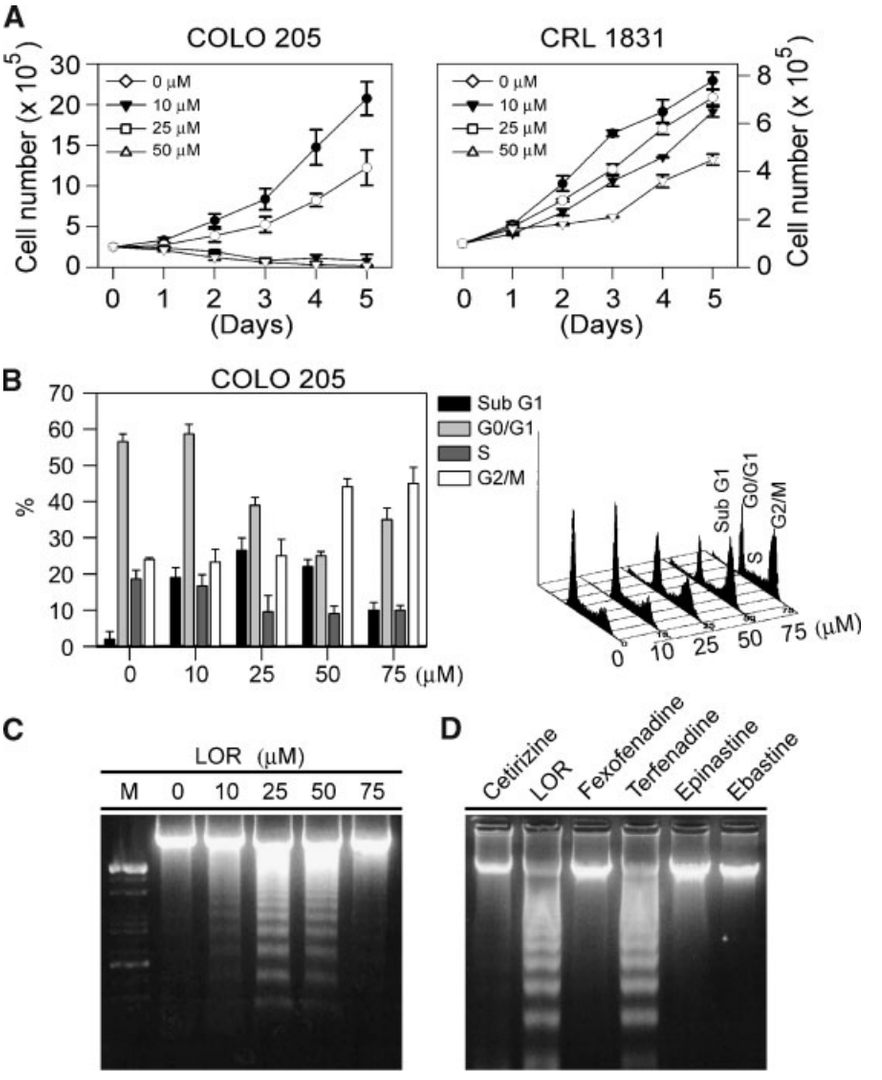

Figure 1. Cell growth inhibitory effects of LOR on human colon cancer and normal epithelial cells. (A) Human colon cancer (COLO 205) cells and human normal CRL 1831 were treated with various concentrations of LOR (10–50 μM) for 5 days. Media with or without LOR were changed everyday until cell counting. Three samples were analyzed in each group and the results were presented as means ± SE. (B) Dose-dependent response of LOR on cell-cycle regulation. COLO 205 cells were cultured in media supplemented with 10% FCS and LOR (10–75 μM) for 24 h. Percentage of cells in sub-G_1, G_0/G_1, S, and G_2/M phases of the cell cycle were determined using established CellFIT DNA analysis software. Three samples were analyzed in each group, and values were presented as mean ± SE. (C) COLO 205 cells were treated with LOR (10–75 μM) or DMSO (0.05%), and DNA fragmentation assay performed 24 h later. M, molecular weight marker. (D) COLO 205 cells were cultured in media supplemented with 10% FCS in the presence of histamine H1 receptor antagonists namely LOR, TF, cetirizine, ebastine, epinastine, and fexofenadine (75 μM each treated for 24 h). DNA fragmentation analysis was then performed as described above.

mitosis. In this study, our results indicated that cells arrested at the G_2/M phase by 24 h of LOR (10–75 μM) treatment were regulated by inhibition of the cyclin B1/cdc2 protein levels and its kinase activity (Figure 2B). In order to examine the time-dependent effect of LOR on G_2/M phase cell-cycle arrest, the COLO 205 cells were synchronized at the G_0/G_1 phase by 0.04% serum starvation for 24 h [25,26]. After serum starvation, the complete medium containing 10% FCS was then replaced. The time points according to Figure 2A and our previous studies [26,41] were selected as 0 h (representing the G_0/G_1 phase), 15 h (representing the S phase), 18 h (representing the G_2/M phase), and 24 h (representing the 2nd G_0/G_1 phase). The cell lysates were then analyzed for expression of cell-cycle regulatory proteins by immunoblotting using specific antibodies (Figure 2C). To assess the Cdc2 kinase activity, the level of phosphorylated Cdc2 (Tyr-15) as well as the level and/or kinase activity of the Wee1 and Cdc25C phosphatase, two key enzymes that regulate the Cdc2 kinase activity, were determined in the

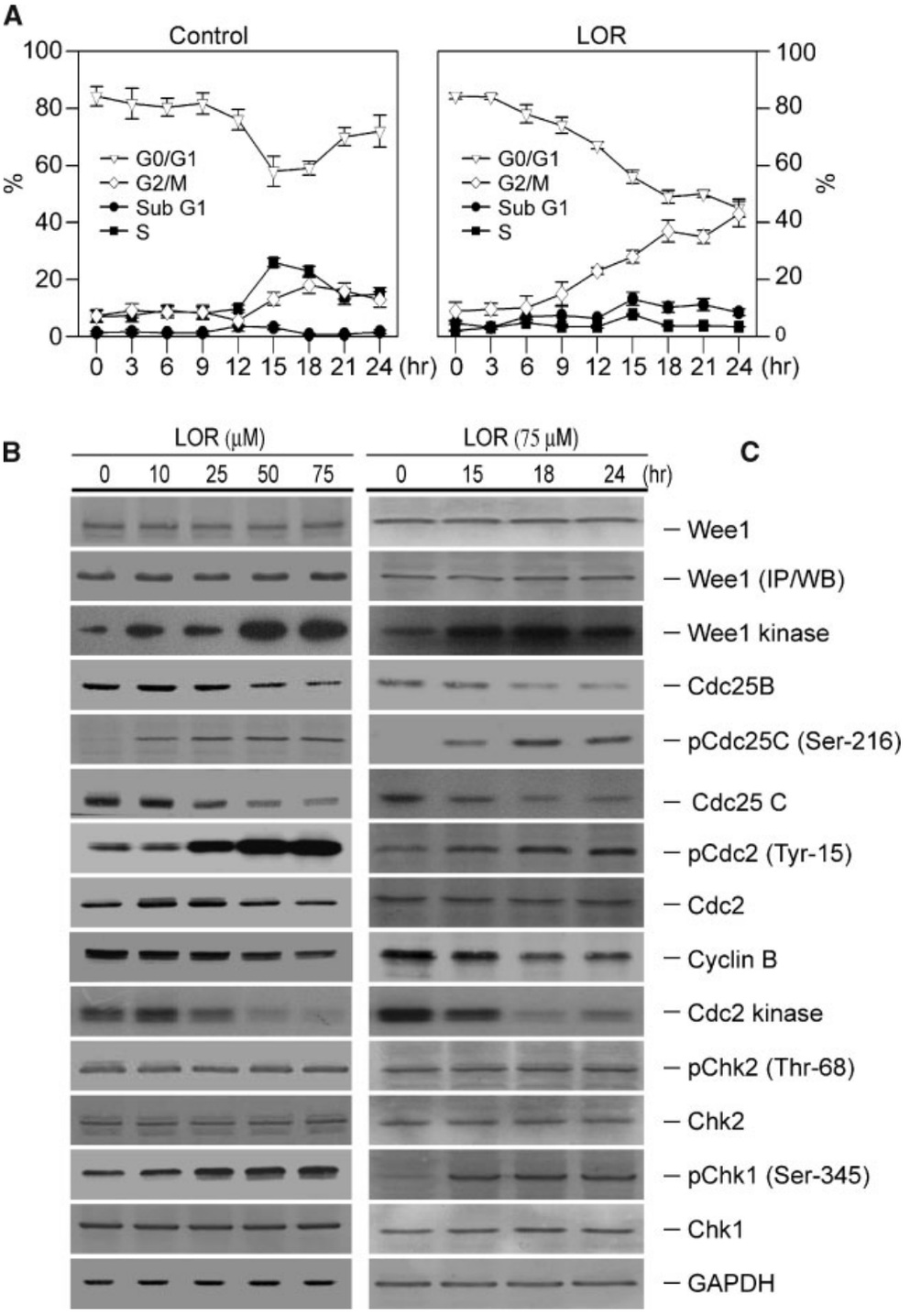

Figure 2. Effects of LOR on cell-cycle regulations in human COLO 205 cells. (A) Time-dependent effects of LOR in human COLO 205 cell-cycle analysis. FACS analysis of DNA content was conducted after COLO-205 cells release from quiescence by incubation in culture media supplemented with 10% FCS in the presence of 0.05% DMSO or LOR (75 μM) at the indicated time points. Percentage of cells in different phases of cell cycle was determined using established CellFIT DNA analysis software. Three samples were analyzed in each group, and values represent the mean ± SE. (B) Dose-dependent effects of LOR on the expression of G_2/M phase regulatory proteins in COLO 205 cells. The cells were rendered quiescent by incubation for 24 h in the cultured media containing 0.04% FCS. After 24 h, cells were released from quiescence by incubation in culture media supplement with 10% FCS and 0.05% DMSO with or without LOR (10–75 μM) for additional 24 h. The cells were harvested, lysed, and the levels of G_2/M phase regulatory proteins and its kinase activities were determined as described in the Materials and Methods. Membrane was also probed with anti-GADPH antibody to correct for difference in protein loading.

LOR-treated COLO 205 cells. The results indicated that phosphorylation of Cdc2 (Tyr-15) and its kinase activity was changed as early as 15 h after LOR (75 μM) treatment (Figure 2C). Consistent with the effect on phosphorylation of Cdc2 (Tyr-15), LOR treatment also resulted in a marked induction of Wee1 kinase activity in the same levels of total Wee1 protein (Figure 2B and C). In addition, the LOR treatment in COLO 205 cells also resulted in a significant reduction in Cdc25C protein levels (Figure 2B and C). Thus, the induction of Wee1 kinase at 15 h after LOR (75 μM) treatment in COLO 205 cells was associated with the decreased of the Cdc25C phosphatase activity which eventually increased the level of phosphorylated Cdc2 (Tyr-15) (Figure 2C). The net effect of the results is a G_2/M arrest following LOR treatment.

Chk1 and Chk2 are intermediaries of DNA damage checkpoints and activated by phosphorylation on Ser-345/Ser-317 and Thr-68, respectively [20,42]. The Chk1 and Chk2 kinases have been reported to inhibit Cdc25C kinase activity by phosphorylation at the Ser-216 residue [43–45]. We therefore examined whether LOR treatment affects the phosphorylation of Chk1 or Chk2. Representative immunoblots for phospho-Chk1 showed increased Ser-345 phosphorylation of Chk1 at 15 h after LOR (75 μM) treatment, whereas the level of total Chk1 proteins were not affected (Figure 2C). The total and its phosphorylated form of the Chk2 (Thr-68) proteins did not changed in the COLO 205 cells even at 24 h after LOR (75 μM) treatment (Figure 2B and C).

To investigate the early stage responses of the COLO 205 cells for LOR treatment, the total and its phosphorylated form of the Chk1 (Ser-345), Chk2 (Thr-68), and Bad (Ser-155) were then determined. As shown in the Figure 3A, our study demonstrated that Chk1 (Ser-345) but not Chk2 (Thr-68) was phosphorylated in the COLO 205 cells as early as 1 h when exposed to higher dose LOR (75 μM). The kinase activity of Chk1 was then determined in the lysates prepared from DMSO- and LOR-treated cells (75 μM for 4 h) using GST-Cdc25C as a substrate. As can be seen in the Figure 3B, the Chk1 kinase activity was significantly higher in LOR-treated cells than in control cells.

The Chk1 is a serine-threonine kinase that is critical for G_2/M arrest in response to DNA damage. Recently, it has been demonstrated that Chk1 inactivate the pro apoptotic protein BAD by phosphorylating residues critical for BAD functions in vitro [46]. In this study, our results demonstrated that BAD (Ser-155) was phosphorylated as early as 1 h in COLO 205 cells by LOR treatment (Figure 3A). Because phosphorylation of Cdc25C (Ser-216) [43] and BAD (Ser-155) [47] creates a binding site for 14-3-3, we then examined the effect of LOR on the binding of Cdc25C and BAD with 14-3-3 (Figure 3C). The lysate proteins from control and LOR-treated cells (10–75 μM for 4 h) were immunoprecipitated using anti-14-3-3 antibody, and the immune complex was analyzed for the presence of Cdc25C and BAD by immunoblotting. As can be seen in Figure 3C, LOR treatment resulted in increased binding of Cdc25C and BAD with 14-3-3 at the 4 h time point. These results suggested that LOR treatment might lead to translocation of Cdc25C from the nucleus to the cytoplasm because of increased binding with 14-3-3. We examined this possibility by immunohistochemistry, and the data were shown in Figure 3D. Cells were treated with DMSO (control) or 75 μM LOR for 4 h, and then stained with anti-pCdc25C (Ser-216) antibody (FITC, green) or nucleic acid binding dye P.I., red. In LOR (75 μM, 4 h)-treated cells, pCdc25C (Ser-216) was localized in the cytoplasm (green staining surrounding P.I.-stained nuclei) as well as in the nucleus (red staining in nucleus). In contrast, the nuclei of the control cells were stained with pCdc25C (Ser-216) (green), indicating translocation of pCdc25C (Ser-216) from the nucleus to the cytoplasm (Figure 3D). Cytoplasmic accumulation of pCdc25C (Ser-216) upon treatment with LOR was confirmed by biochemical fractionation of cytoplasmic, and nuclear fractions from control (DMSO-treated) and LOR treated (75 μM for 4 h) cells followed by immunoblotting using anti-pCdc25C (Ser-216) antibody, and the results were shown in Figure 3E. The total protein level of Cdc25C was also determined in different fractions of the LOR- and control-treated cells, which represented as a protein loading control. A 4 h time point was selected to minimize influence of LOR induced decline in

Figure 3. Effect of LOR on binding of Cdc25C and BAD with 14-3-3 and on nuclear/cytoplasmic distribution of Cdc25C. (A) Immunoblotting assay for effect of LOR on protein level, and phosphorylation of Chk1 (Ser-345) and BAD (Ser-155). COLO 205 cells were cultured in the presence of 75 μM LOR for the indicated time periods. The blots were stripped and reprobed with anti-GAPDH antibody to ensure equal protein loading. (B) Effect of LOR on Chk1 kinase activity. COLO cells were treated with DMSO or 75 μM LOR for 4 h. Chk1 was immunoprecipitated from the lysates of control and LOR-treated cells, and the kinase activity was determined using synthesized Cdc25C peptide as a substrate described in Materials and Methods. The membrane was probed with anti-Chk1 antibody to ensure equal protein loading. (C) Effect of LOR on binding of phosphor Cdc25C (Ser-216) and phosphor BAD (Ser-155) with 14-3-3. The protein lysates (200 μg) from control and LOR-treated cells (10–75 μM for 4 h) were used for immunoprecipitation with anti-14-3-3 antibody followed by Western blotting (WB) for phosphor Cdc25C (Ser-216) and phosphor BAD (Ser-155). (D) Confocal microscopic analysis for nuclear/cytoplasmic distribution of Cdc25C (Ser 216) in control (DMSO-treated) and LOR-treated cells. Cells were treated with DMSO (control) or 75 μM LOR for 1 or 4 h and then stained with anti-Cdc25C (Ser-216) antibody (green) or P.I. (red). (E) Immunoblotting assay for pCdc25C(Ser-216) and Cdc25C using nuclear and cytoplasmic fractions prepared from control (DMSO-treated) and LOR-treated cells (75 μM for 4 h). Blots were stripped and reprobed with anti-β-actin and anti-PCNA antibodies to normalize for equal protein loading as well as to rule out cross contamination of the nuclear and cytoplasmic fractions. [Color figure can be viewed in the online issue, which is available at www.interscience.wiley.com.]

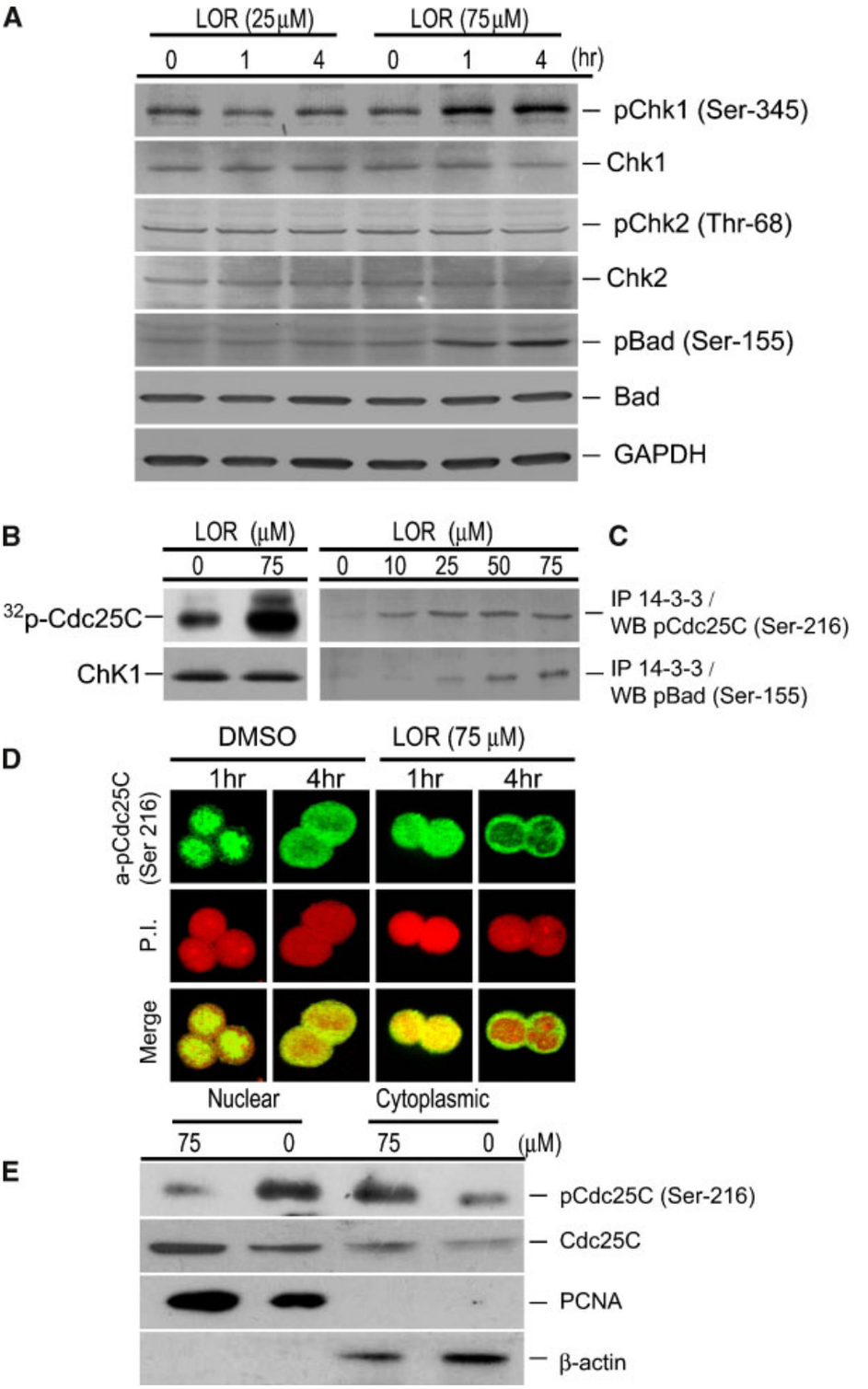
A
LOR (25μM)
LOR (75μM)
0 1 4 0 1 4 (hr)
pChk1 (Ser-345)
Chk1
pChk2 (Thr-68)
Chk2
pBad (Ser-155)
Bad
GAPDH
B
LOR (μM)
0 75
32p-Cdc25C
ChK1
C
LOR (μM)
0 10 25 50 75
IP 14-3-3 /
WB pCdc25C (Ser-216)
IP 14-3-3 /
WB pBad (Ser-155)
D
DMSO
LOR (75 μM)
1hr 4hr 1hr 4hr
a-pCdc25C (Ser 216)
P.I.
Merge
E
Nuclear
Cytoplasmic
75 0 75 0 (μM)
pCdc25C (Ser-216)
Cdc25C
PCNA
β-actin

Figure 3.

Cdc25C protein level shown in the Figure 2B. In DMSO-treated control, the intensity of Cdc25C immunoreactive band was significantly higher in the lane corresponding to nuclear fraction than in the cytoplasmic fraction (Figure 3E). Treatment of cells with LOR (75 μM) resulted in a decrease in nuclear Cdc25C signal intensity with a concomitant increase in cytoplasmic Cdc25C signal intensity (Figure 3E). The blot was stripped and reprobed with anti-β-actin and anti-PCNA antibodies to determine cross contamination, if any, of the nuclear and cytoplasmic fractions and to ensure equal protein loading (Figure 3E). These results confirmed that LOR treatment, indeed, promoted translocation of Cdc25C from the nucleus to the cytoplasm.

To determine the possible role of Chk1 kinase activation in the regulation of LOR-mediated G_2/M arrest, we examined the effects of Chk1 kinase on LOR-induced G_2/M arrest in COLO 205 cells using Chk1-specific inhibitor SB-218078 [21]. We first demonstrated that SB-218078 (0.1 μM) inhibited the phosphorylation of Chk1(Ser-345) and its kinase activity in COLO 205 cells when treated with LOR (Figure 4A). The inhibitory effects of SB-218078 on LOR-induced Cdc25C, Cdc2, and BAD phosphorylation were demonstrated (Figure 4A). To determine the effective dose of SB-218078 on LOR-mediated G_2/M arrest response, COLO 205 cells were treated with LOR and then cultured for 24 h in the presence of SB-218078 (0.1 and 1 μM). The resulting cells were analyzed for DNA contents by FACS flowcytometric analysis as described in Materials and methods. The results showed that the LOR-induced G_2/M arrested cells (Figure 4B, solid bar) was 3.9-fold higher than that in the control cells (Figure 4B, open bar). Furthermore, incubation of LOR-treated COLO 205 cells with SB-218078 resulted in a marked attenuation of LOR-induced G_2/M arrest in a dose-dependent manner (Figure 4B, solid bars). Incubation with 0.1 μM SB-218078 inhibited the LOR-induced G_2/M arrest by approximately 50%, while incubation with 1 μM SB-218078 diminished the LOR-induced G_2/M cell-cycle arrest by 80% (Figure 4B, solid bars). No further inhibitory effect on LOR-induced G_2/M arrest was seen when higher doses of SB-218078 were used (data not shown). Incubation of DMSO-treated COLO 205 cells with SB-218078 had no detectable effect on the population of cells containing 4N-DNA (G_2/M phase cells) (Figure 4B, open bars).

To further clarify the role of checkpoint kinases activation on LOR-mediated G_2/M arrest, two inhibitors were adapted in our experiment including DBH [48] and caffeine [49–51], which inhibited the Chk1/Chk2 and ataxia telangiectasia-mutated (ATM)/ATR kinases, respectively. Interestingly, the LOR-mediated G_2/M arrest was completely attenuated by DBH (10 μM) (Figure 4C, gray bars), but not by caffeine (5 mM) (Figure 4C, open bars). Such results implied that at least part of the LOR-induced G_2/M arrested cells utilize a caffeine-insensitive pathway in which checkpoint signaling by ATM or ATR was most likely not involved.

To examine the effect of Chk1 on LOR-mediated apoptotic effects, COLO 205 cells were treated with LOR (25 and 75 μM) and then incubated for 24 h in the medium containing 0.1–1 μM SB-218078 (Figure 4D, lanes 5 and 6) or, as a control, 0.05% DMSO (Figure 4D, lane 1). The presence of DNA fragmentation was detected as described above. The dose of SB-218078 used in this study (0.1–1 μM) was found to maximally prevent the LOR-induced G_2/M arrest, which resulted in DNA laddering formation (Figure 4D, lanes 5 and 6). As a control, a parallel set of COLO 205 cells was incubated in the presence of 1 μM SB-218078, no significant DNA fragmentation was observed (Figure 4D, lane 2).

Our results revealed that lower dose (10–50 μM) LOR could induced both the G_2/M arrest and apoptosis in COLO 205 cells (Figure 1B and D). The mechanisms of LOR-mediated apoptosis need to be further investigated. Since the mitochondria signaling regulatory proteins seems to be required for different anti-cancer agents-induced apoptosis in COLO 205 cells [35,52–54]. We first examined whether cytochrome C release from mitochondria into the cytosol and dissipation of the electrochemical gradient ($\Delta\Psi$m) was involved in the LOR-mediated apoptosis. This was monitored by staining the COLO 205 cells with JC-1, a fluorescent dye, which differentially stains mitochondria in accordance to their $\Delta\Psi$m. Active mitochondria with high $\Delta\Psi$m accumulate JC-1 aggregates, which are red (Figure 5A, 0 h), whereas, in the mitochondria with low $\Delta\Psi$m, JC-1 stays in a monomeric, green form (Figure 5A, 12 h). This renders the red/green ratio, a

Figure 4. The Chk1 regulatory effects of LOR-induced G_2/M cell cycle arrest. (A) COLO 205 cells were treated with LOR (75 μM) in the presence of SB-218078 (0.1 and 1 μM) for 24 h. The treated cells were collected, lysed, and the level of phosphorylated Chk1 (Ser-345), Cdc25C (Ser-216), Cdc2 (Tyr-15), and BAD (Ser-155) as well as the level of total Chk1, Cdc25C, Cdc2, and BAD in each sample was determined by immunoblotting analysis with relevant specific antibodies. The Chk1 kinase activity was determined as described in Materials and Methods. (B) Cells were treated with DMSO (open bars) or LOR (75 μM) (solid bars), and incubated for 24 h in the presence of Chk1 inhibitor (SB-218078). The resulting cells were harvested, stained with PI and analyzed for DNA contents by flowcytometry as described above. Percentage of cells with 4N-DNA content, indicative of G_2/M phase of the cell cycle, is shown as the mean ± SE from three independent experiments. (C) COLO 205 cells were treated with LOR (75 μM) followed by incubation for 24 h in medium containing 0.05% DMSO (solid bars), 5 mM caffeine (open bars), or 10 μM DBH (gray bars). Cell samples were analyzed for DNA content by flowcytometry. The percentage of G_2/M phase cells shown represents the average of three independent experiments. (D) COLO 205 cells were incubated for 24 h in medium containing 0.05% DMSO, SB-218078 alone, or combine treatment with LOR and SB218078. The DNA samples were isolated from cells and analyzed for DNA fragmentation as described in the Material and Methods.

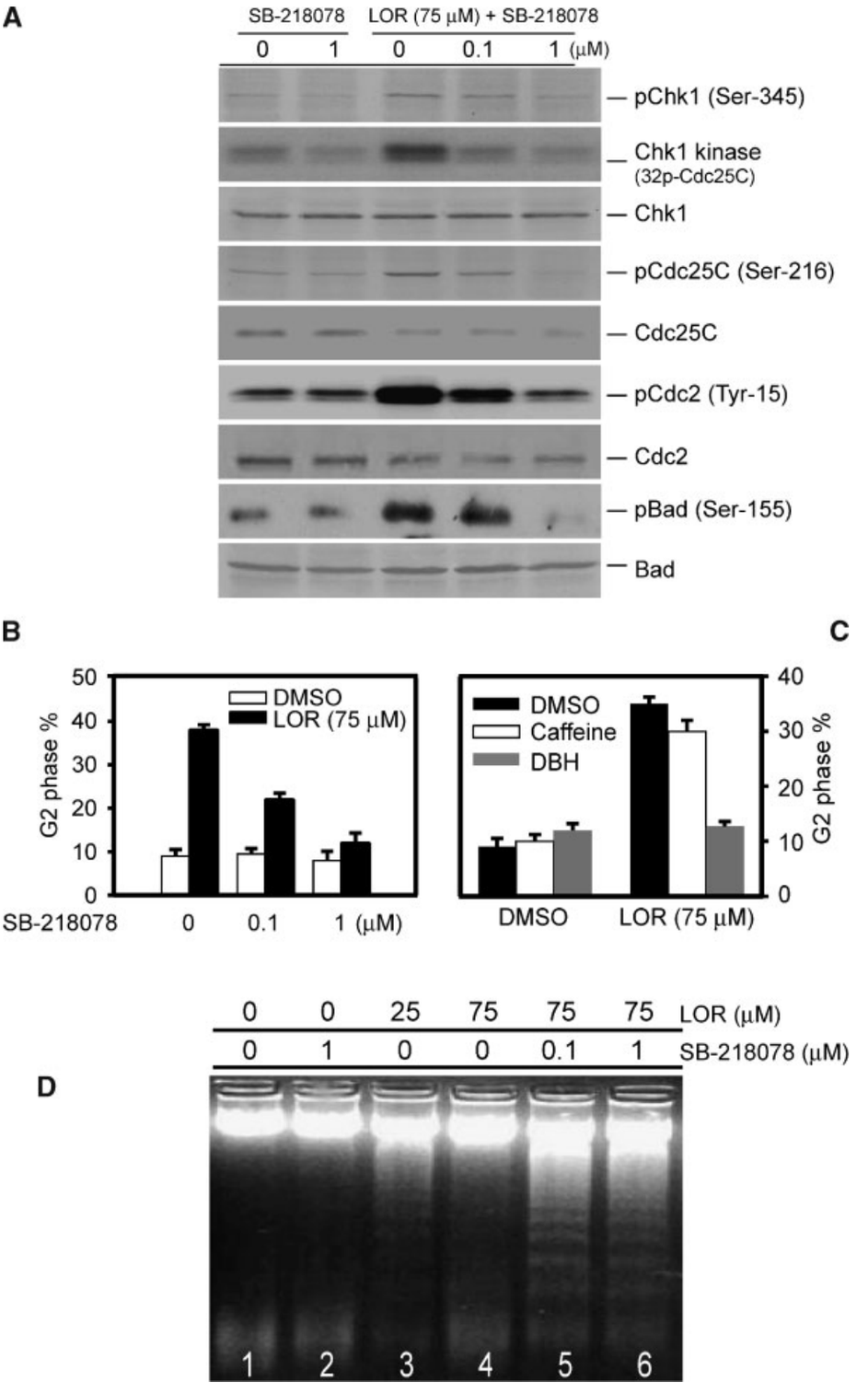
A
SB-218078
LOR (75 μM) + SB-218078
0 1 0 0.1 1 (μM)
pChk1 (Ser-345)
Chk1 kinase
(32p-Cdc25C)
Chk1
pCdc25C (Ser-216)
Cdc25C
pCdc2 (Tyr-15)
Cdc2
pBad (Ser-155)
Bad
B
G2 phase %
DMSO
LOR (75 μM)
SB-218078 0 0.1 1 (μM)
C
DMSO
Caffeine
DBH
G2 phase %
DMSO LOR (75 μM)
D
0 0 25 75 75 75 LOR (μM)
0 1 0 0 0.1 1 SB-218078 (μM)
1 2 3 4 5 6

Figure 4.

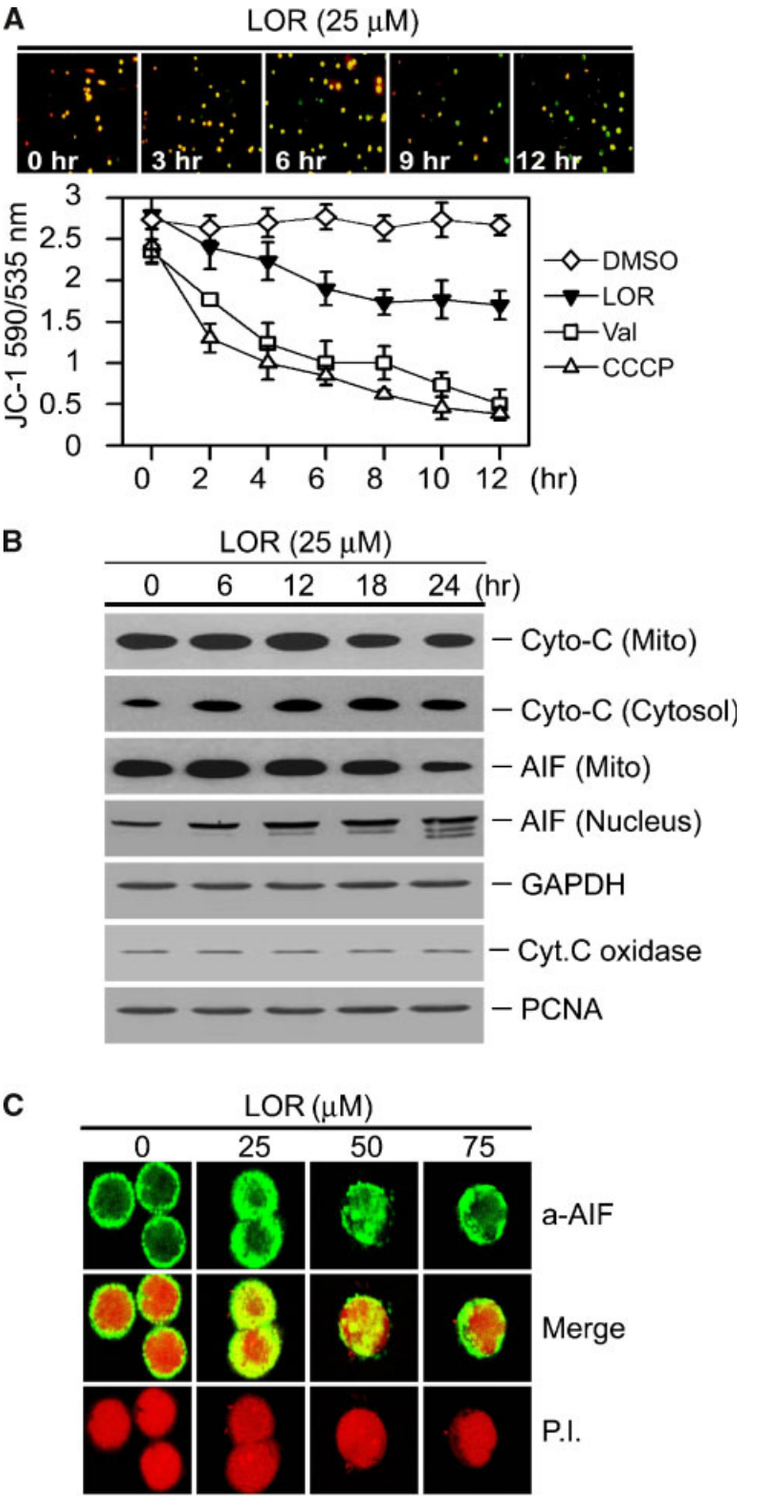
A
LOR (25 μM)
0 hr
3 hr
6 hr
9 hr
12 hr
JC-1 590/535 nm
3
2.5
2
1.5
1
0.5
0
0 2 4 6 8 10 12 (hr)
DMSO
LOR
Val
CCCP
B
LOR (25 μM)
0 6 12 18 24 (hr)
Cyto-C (Mito)
Cyto-C (Cytosol)
AIF (Mito)
AIF (Nucleus)
GAPDH
Cyt.C oxidase
PCNA
C
LOR (μM)
0 25 50 75
a-AIF
Merge
P.I.

Figure 5.

sensitive indicator of the mitochondrial $\Delta\Psi m$ changes, which does not depend on other factors such as mitochondrial size, shape, and density, which may influence single-component fluorescent signals. Analyzed in a real-time plate reader assay, $\Delta\Psi m$ stayed relatively stable in untreated COLO 205 cells, while it was rapidly (within 6 h) dissipated by 25 μM LOR treatment (Figure 5A, lower panel). The $\Delta\Psi m$ was rapidly (within 2 h) dissipated by the uncoupler CCCP or by the K^+ ionophore Val and served as a positive control (Figure 5A). As shown in the Figure 5A and B, we found that LOR (25 μM) increased outer (cytochrome C and AIF release) and inner (loss of $\Delta\Psi m$) mitochondria membrane permeability. The release of cytochrome C and AIF were then observed as early as 6 h which kinetically paralleled a decreased of mitochondria membrane potential (Figure 5A and B). These observations suggest that LOR-induced apoptosis may be initiated with early alterations in mitochondrial membrane stability.

As shown in the Figure 5B, the AIF was released from mitochondria and translocated into nucleus as early as 6 h after LOR treatment in the COLO 205 cells. To our knowledge, AIF was demonstrated to be involved in initiate the nuclear apoptotic events including nuclear membrane degradation, peripheral chromatin condensation, large-scale fragmentation of DNA, and, ultimately, cytotoxicity [55]. We then confirmed the LOR-induced nuclear translocation of the AIF by immunofluorescence staining observed by confocal microscopic analysis. In consistent to the result shown in Figure 5B, our data demonstrated that AIF translocation to nucleus was found in COLO 205 cells at 6 h after LOR (25–50 μM) treatment. As shown in the Figure 5C, the AIF translocation to nucleus was not observed in COLO 205 cells after treated with higher dose of LOR (75 μM). Similar result was observed in the Figure 1B indicated that LOR-induced DNA fragmentation was not observed in the COLO 205 cells when exposed to higher dose (75 μM) LOR. Such observations indicating that higher dose LOR may trigger some mediators which induced G_2/M cell growth arrest effects and may contribute to inhibit of cellular apoptosis stress sensing.

To investigate the molecular events of LOR-induced apoptosis, we then investigated the apoptotic responses by which the initiator (caspase 9 and 8) and the effector (caspase 3) were determined by immunoblotting and caspase activity analysis (Figure 6A and B). The COLO 205 cells were treated with various concentrations of LOR (10–75 μM) for 24 h. Our data demonstrated that LOR at a lower dose (25–50 μM) activated the caspase 3 as evidenced by a decreased in the protein level of procaspase 3 and degradation of the poly-ADP-ribose polymerase (PARP), the substrate for caspase 3 (Figure 6A). To further elucidate the apoptotic pathways involved in the activation of caspase 3, we examined the changes of the protein levels of caspases 8 and 9 in the LOR-treated COLO 205 cells. Treatment of COLO 205 cells with LOR (25–50 μM) resulted in caspase 9 activation evidenced by degradation of the procaspase 9 but not by caspase 8 because substrate of the caspase 8 (truncated form of Bid, t-Bid) was not degraded (Figure 6A). These observations suggest that LOR-induced apoptosis is dependent on caspase 9 activation. Activation of caspase 9 in the Apaf-1 apoptosome is predominantly triggered by the release of cytochrome C from mitochondria into the cytoplasm [56]. Accordingly, the cytosolic and mitochondrial fractions, prepared from cells treated with LOR (25 μM) time-dependently were subjected to Western blot analysis to assess the release of cytochrome C and demonstrated that the LOR induced a significant increase in cytosolic levels of cytochrome C as early as 6 h after LOR treatment (Figure 5B). To further confirm the Western blot results, we performed caspase activity assays. As shown in Figure 6B, treatment of COLO 205 cells with 25 μM LOR induced caspase 3 activity about 7.8-folds and 11.2-folds at 9 and 12 h compared to control, respectively, while induced caspase 9 activity about 5.1-folds and 7.8-folds at 9 and 12 h compared to control, respectively. We therefore hypothesized that LOR-mediated apoptosis was through the mitochondria signaling pathways in which the caspase 9 protein may be activated.

We next examined the therapeutic efficacy of LOR (25 mg/Kg) in vivo by treating athymic nude mice bearing COLO 205 tumor xenografts. After establishment of palpable tumors (mean tumor volume, 200 mm^3), animal received I.P. injections of LOR three times per wk, as well as DMSO plus peanut oil as a vehicle control. After 6 wks, gross morphology of

Figure 5. Evaluation on the role of the mitochondria signals involved in LOR induced apoptosis. (A) The top insets, mitochondria membrane depolarization in LOR-treated COLO 205 cells was measured by JC-1 staining. In the lower panel, COLO 205 cells were treated with LOR (25 μM), Val (200 μM), or with CCCP (200 μM) for the indicated time points. After drug treatment, the COLO 205 cells were stained with JC-1 (1 μg/ml) as described in Materials and Methods. Results were expressed as a change in the ratio between red JC-1 fluorescence (Em 590 nm) and green JC-1 fluorescence (Em 535 nm) over time. Each point represents the mean ± SE from three independent experiments. (B) COLO 205 cells were treated with LOR (25 μM) time dependently. The protein level of the cytochrome C and AIF released form mitochondria into the cytoplasmic and nuclear were then determined by Western blot analysis. The expression levels of the cytochrome C oxidase (subunit IV), GAPDH, and PCNA proteins were employed as a loading control to rule out cross contamination of the mitochondria, cytoplasmic, and nuclear fractions, respectively. (C) Confocal microscopic analysis for nuclear/cytoplasmic distribution of AIF in control (DMSO-treated) and LOR-treated cells. Cells were treated with DMSO (control) or LOR (25–75 μM) for 4 h and then stained with anti-AIF antibody (green) or P.I. (red). [Color figure can be viewed in the online issue, which is available at www.interscience.wiley.com.]

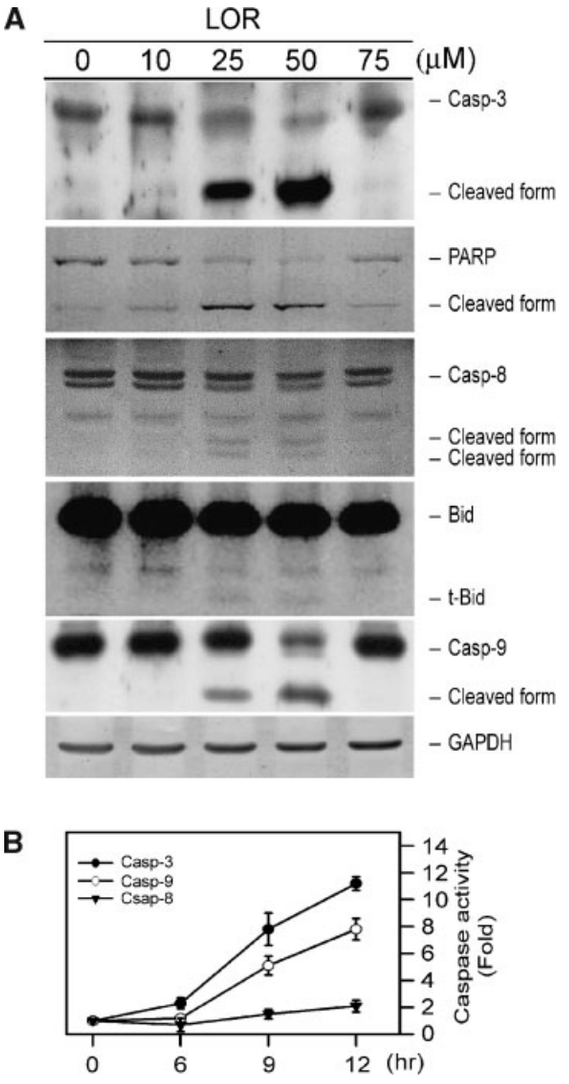

Figure 6. Dose-dependent response of caspase activity involved in LOR-mediated apoptosis in COLO 205 cells. (A) COLO 205 cells were treated with LOR (10–75 μM) for 24 h and the expression levels of caspase-associated proteins were determined by Western blot analysis. The expression level of the GAPDH protein was selected and as a loading control. (B) COLO 205 cells were treated with 25 μM LOR for the indicated time points. The LOR-induced caspase activities in COLO 205 cells were measured as described in Materials and Methods. Data was represented as mean ± SE from three independent determinations.

the tumor volume in mice treated with LOR (Figure 7A, mice No. 5–8) was significant smaller in comparison with DMSO-treated controls (Figure 7A, mice No. 1–4). A reduction in tumor volume between mice given LOR versus those given vehicle (DMSO) was detected (Figure 7B–E). In mice receiving these treatment regimens, no gross signs of toxicity were observed (body weight, visible inspection of general appearance, and microscopic examination of individual organs). Our results provide further evidences that such observations may have significance of application for cancer chemotherapeutic purposes.

DISCUSSIONS

LOR, which is a promising world widely used oral-anti-histamine agent, has been used in the treatment of allergic disease. In this study, we have shown that LOR effectively inhibits proliferation of human colon cancer (COLO 205) cells by causing G_2/M cell-cycle arrest and caspase 9-mediated apoptosis. In vivo study revealed that the growth of COLO 205 xenografts in nude mice was retarded significantly upon I.P. administration of LOR with a clinical therapeutic relevance dose (25 mg/kg). These results prompted us to examine further the mechanisms by which LOR inhibits proliferation of cancer cells.

Recent studies demonstrated that cells response to DNA damage agents initiated two distinct checkpoint kinases namely Chk1 and Chk2 [18,57]. Recently, several Chk1 and Chk2 checkpoint abrogating agent (abrogator) have been developed as adjuvants and intended to improve the therapeutic index of cancer chemotherapy [23,58]. The original studies were performed by using caffeine, a non-specific G_2 abrogator which disrupt the G_2 checkpoint to sensitize G_1-defective cancer cells into apoptosis [59,60]. In our study, the Chk1 specific inhibitor (SB-218078) were used as a G_2 phase abrogator and demonstrated that SB-218078 abrogate the LOR-induced G_2/M arrest and sensitized the cells from G_2/M arrest into apoptosis (Figure 4D). Additional studies also demonstrated that knock-down of Chk1, Wee1, and Myt1 by RNA interference abrogates either adriamycin- or paclitaxel-mediated G_2 checkpoint and induces apoptosis in human cancer cells [17,58,61]. Therefore, Chk1 downregulation can not only potentiate DNA-damaging agents, but also enhance the toxicity of anti-microtubule agents (such as paclitaxel) [12,17,58], which significantly broadens its therapeutic applications.

In our study, the LOR-induced G_2/M phase arrest was completely attenuated by SB218078 and DBH but not by caffeine (Figure 4B). Caffeine has been shown to inhibit the activities of both ATM and ATR upstream checkpoint kinases and to override the ATM- and ATR-dependent DNA damage checkpoints [49]. Recently, a cell-free experimental system from *Xenopus* eggs extracts was performed and described a caffeine-insensitive pathway which plays some important role in the checkpoint response [62,63]. Similar reports in human colon cancer cells also demonstrated that ATR-mediated DNA-damage checkpoint was not completely rescued by caffeine. For example, increased phosphorylation of γH2AX was regulated by ATR in response to DNA breaks observed in human colon cancer cells [64]. The phosphorylated γH2AX was also induced in human colon cancer (HCT 116) cells by DNA alkylating agent, hedamycin. In this study, caffeine did not

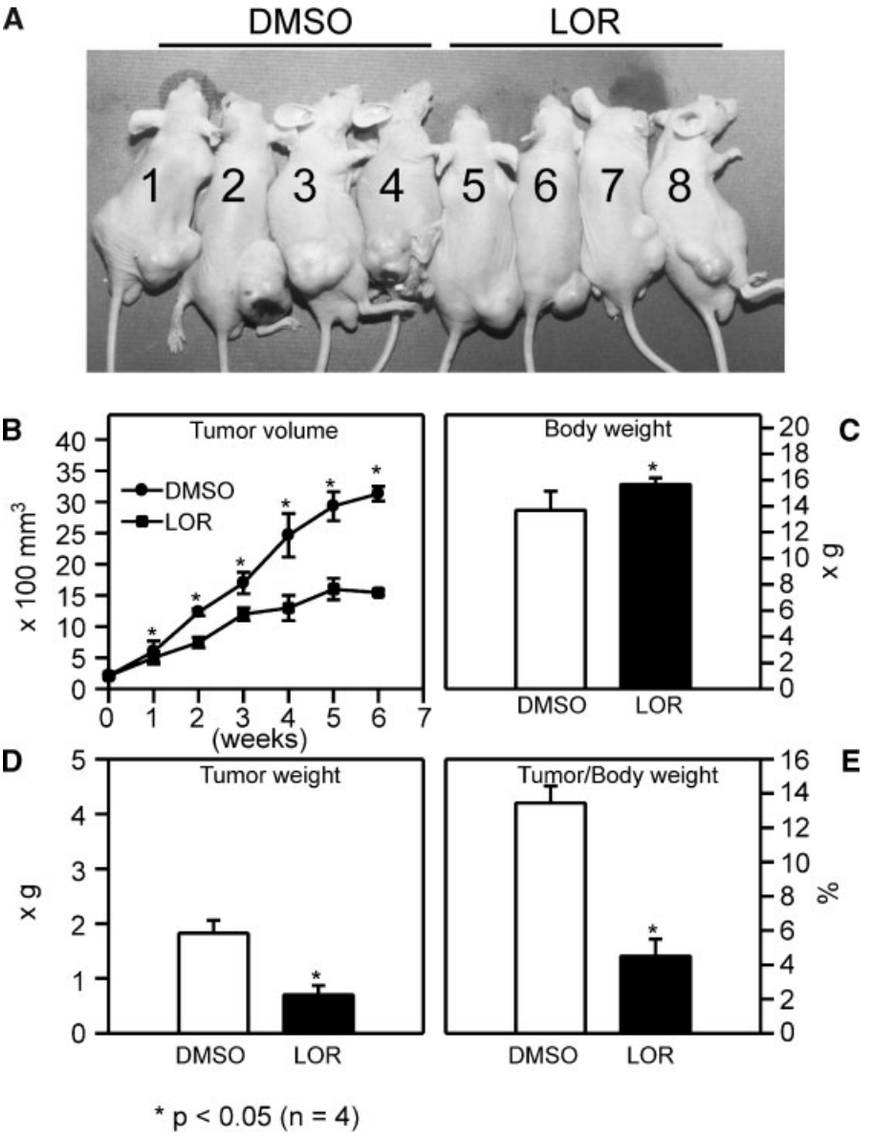

Figure 7. The growth of COLO 205 tumor xenografts in nude mice was retarded by LOR treatment. Athymic nude mice injected with COLO 205 cells into subcutaneous tissue of inter-scapular area. Once tumor volume reached approximately 200 mm^3, the animal received treatment of 25 mg/kg LOR, or DMSO intraperitoneally three times per wk for 6 wk. (A) Gross appearance of subcutaneous tumors after treatment with DMSO (shown as No. 1–4) or LOR (shown as No. 5–8) for 6 wk. (B) Average tumor volume of DMSO-treated (circle) versus LOR-treated (square) nude mice, (C) body weight, (D) tumor weight, and (E) tumor/body weight ratio were measured at the end of the experiment. Four samples were analyzed in each group and values represent the mean ± SE. Comparisons were subjected to Student's *t* test. $^*P < 0.05$ versus control.

substantially reduce induction of H2AX phosphorylation by hedamycin [65]. The H2AX phosphorylation was also induced by silibinin, a naturally occurring flavonoid, which against ultraviolet B (UVB)-induced skin tumorigenesis. However, the anti-tumor effects of silibinin is possibly not through ATM/ATR activation, as caffeine pretreatment had no effect on silibinin plus UVB induced p53-Ser15 phosphorylation [66].

As described above, caffeine is a well-known inhibitor of both ATM and ATR pathways, it could not completely reverse the LOR-induced G_2/M arrest (Figure 4C). These results suggest that a caffeine-sensitive pathway responsible for maintenance of the LOR-induced G_2/M-arrested cells is dependent on both ATR and Chk1 checkpoint kinases. In such a situation, the G_2/M arrest induced by LOR can be prevented by caffeine pretreatment. However, our data indicated that at least part of LOR-induced G_2/M arrested cells utilize a caffeine-insensitive pathway, that is, that checkpoint signaling by ATM or ATR is most likely not involved. This result cannot exclude

a possibility indicated that a distinct, caffeine-insensitive ATM/ATR signaling pathway might also be necessary to attenuate the effects of LOR-mediated G_2/M arrest and also plays a role in the checkpoint response.

In our and others previous studies [12,26,41], the cyclin B1 protein was induced in the microtubule damaging agents-mediated G_2/M arrested cells due to block of the mitotic process. However, decreased of cyclin B1 protein level was also observed in the G_2/M arrested cells through inhibition of the mRNA synthesis and accelerate degradation of the cyclin B1 protein [5,67–69]. The cyclin B1 suppression probably prevents the optimal formation of the mitosis- or maturation-promoting factor (MPF) which consists of a complex between the cyclin B1 and the Cdc2 kinase protein, and is essential for cells to cross the threshold from G_2 into mitosis. In this study, our results revealed that cyclin B1 inhibition and its inactivation of the cyclinB1/Cdc2 kinase activity may be play an essential role in LOR-induced G_2/M arrest. Such hypothesis has also been proposed in previous studies revealed that cyclin B1 expression in human cancer cells was inhibited by different stimulations including ionizing radiation [70], DNA damaging agents [67], or cancer chemopreventive agents [5,71,72]. In addition, recent studies have shown that ectopic expression of BRCA1 in human cells can trigger cellular responses including G_2/M cell cycle arrest and apoptosis [68,69]. The BRCA1 regulates the G_2/M checkpoint was also demonstrated by activating Chk1 kinase and inhibition of cyclin B1 upon DNA damage [69]. Similarly, our findings of decreased cyclin B1 expression concomitant with the induction of Chk1 in the LOR-induced G_2/M arrested cells were in agreement with the data from Yarden et al. (2002) [69].

As described above, the Cdc25C phosphatase is a dual specific phosphatase that triggers the activation of Cyclin B1/Cdc2 by dephosphorylating Cdc2 at the residues Thr-14 and Tyr-15 [73]. The activity of Cdc25C is downregulated by Chk1 kinase through phosphorylation of residue at Ser-216, which affects both the enzyme activity and the subcellular localization of the Cdc25C [74]. Our results indicated that increased phosphorylation of Cdc25C (Ser-216) in response to LOR treatment in the COLO 205 cells was associated with Chk1 activation (Figure 4A). Our results shown in the Figure 3C–E confirmed the previous reports suggested that the Cdc25C is phosphorylated by Chk1 kinase at the Ser-216 residue, which generates consensus binding sites for 14-3-3 proteins and then inactivate the Cdc25C by sequestrate this protein into the cytoplasm [5,69]. Thus, LOR-induced activation of Chk1 is important for the subsequent inactivation of Cdc25C and Cdc2, which eventually caused the G_2/M cell-cycle arrest. The Chk1 has also been demonstrated to inactivate the proapoptotic protein BAD by phosphorylation at the residue of Ser-155 [46], which results in sequestering BAD from mitochondria into cytosol by interacting with 14-3-3 [75]. The LOR-mediated Chk1 kinase activity was inhibited by SB-218078 which prevent the formation of p-BAD/14-3-3 complex and promoted the G_2/M phase arrested cells into apoptosis in the COLO 205 cells (Figure 4A).

In summery, the results of this study provide evidence that LOR-induced G_2/M arrest in COLO 205 cells involves regulation of Cdc2 activity through three distinct mechanisms, which include LOR-induced activation of Chk1 kinase and LOR-induced downregulation of Cdc25C protein levels. Each of these mechanisms results in a decrease in Cdc2 kinase activity. Of particular interest is the finding that the LOR-induced activation of Chk1 is implicated in each of these mechanisms of Cdc2 regulation. Thus, studies in this report indicate that activation of Chk1 plays a central role, either directly or indirectly, in the induction of G_2/M cell-cycle arrest and apoptosis by LOR through alterations in Cdc25C and BAD protein localization and activity. However, our study still needed to address a fundamental question, which remains unanswered, is how LOR treatment causes DNA damage to activate ATR/Chk1. Additional studies needed to identify the specific mechanisms of LOR-mediated activation of Chk1, as well as the precise role of Chk1 on the regulation of G_2/M arrest and apoptosis.

ACKNOWLEDGMENTS

This study was supported by the National Science Council grant NSC 92-2314-B-038-029 to Dr. Ho, and NSC 92-2320-B-038-018 to Dr. Lee.

REFERENCES

1. Hunter T, Pines J. Cyclins and cancer II: Cyclin D and CDK inhibitors come of age. Cell 1994;79:573–582.
2. Huang TS, Shu CH, Chao Y, Chen SN, Chen LL. Activation of MAD 2 checkprotein and persistence of cyclin B1/CDC 2 activity associate with paclitaxel-induced apoptosis in human nasopharyngeal carcinoma cells. Apoptosis 2000;5:235–241.
3. Kharbanda S, Yuan ZM, Taneja N, Weichselbaum R, Kufe D. p56/p53lyn tyrosine kinase activation in mammalian cells treated with mitomycin C. Oncogene 1994;9:3005–3011.
4. Kawabe T, Suganuma M, Ando T, Kimura M, Hori H, Okamoto T. Cdc25C interacts with PCNA at G_2/M transition. Oncogene 2002;21:1717–1726.
5. Singh SV, Herman-Antosiewicz A, Singh AV, et al. Sulforaphane-induced G2/M phase cell cycle arrest involves checkpoint kinase 2-mediated phosphorylation of cell division cycle 25C. J Biol Chem 2004;279:25813–25822.
6. Advani SJ, Brandimarti R, Weichselbaum RR, Roizman B. The disappearance of cyclins A and B and the increase in activity of the G(2)/M-phase cellular kinase cdc2 in herpes simplex virus 1-infected cells require expression of the alpha22/U(S)1.5 and U(L)13 viral genes. J Virol 2000;74:8–15.
7. Dunphy WG. The decision to enter mitosis. Trends Cell Biol 1994;4:202–207.

8. Wilker EW, Grant RA, Artim SC, Yaffe MB. A structural basis for 14-3-3 sigma functional specificity. J Biol Chem 2005; 280:18891–18898.
9. Peng CY, Graves PR, Ogg S, et al. C-TAK1 protein kinase phosphorylates human Cdc25C on serine 216 and promotes 14-3-3 protein binding. Cell Growth Differ 1998;9:197–208.
10. Jiang K, Pereira E, Maxfield M, Russell B, Goudelock DM, Sanchez Y. Regulation of Chk1 includes chromatin association and 14-3-3 binding following phosphorylation on Ser-345. J Biol Chem 2003;278:25207–25217.
11. Lee J, Kumagai A, Dunphy WG. Positive regulation of Wee1 by Chk1 and 14-3-3 proteins. Mol Biol Cell 2001;12:551–563.
12. Xiao Z, Xue J, Sowin TJ, Rosenberg SH, Zhang H. A novel mechanism of checkpoint abrogation conferred by Chk1 downregulation. Oncogene 2005;24:1403–1411.
13. Shao RG, Cao CX, Pommier Y. Abrogation of Chk1-mediated S/G_2 checkpoint by UCN-01 enhances ara-C-induced cytotoxicity in human colon cancer cells. Acta Pharmacol Sin 2004;25:756–762.
14. Suganuma M, Kawabe T, Hori H, Funabiki T, Okamoto T. Sensitization of cancer cells to DNA damage-induced cell death by specific cell cycle G_2 checkpoint abrogation. Cancer Res 1999;59:5887–5891.
15. Xiao Z, Xue J, Semizarov D, Sowin TJ, Rosenberg SH, Zhang H. Novel indication for cancer therapy: Chk1 inhibition sensitizes tumor cells to antimitotics. Int J Cancer 2005;115: 528–538.
16. Jin ZH, Kurosu T, Yamaguchi M, Arai A, Miura O. Hematopoietic cytokines enhance Chk1-dependent G_2/M checkpoint activation by etoposide through the Akt/GSK3 pathway to inhibit apoptosis. Oncogene 2005;24:1973–1981.
17. Ren Q, Liu R, Dicker A, Wang Y. CHK1 affects cell sensitivity to microtubule-targeted drugs. J Cell Physiol 2005;203: 273–276.
18. Huang X, Tran T, Zhang L, Hatcher R, Zhang P. DNA damage-induced mitotic catastrophe is mediated by the Chk1-dependent mitotic exit DNA damage checkpoint. Proc Natl Acad Sci USA 2005;102:1065–1070.
19. Sancar A, Lindsey-Boltz LA, Unsal-Kacmaz K, Linn S. Molecular mechanisms of mammalian DNA repair and the DNA damage checkpoints. Annu Rev Biochem 2004;73: 39–85.
20. Liu Q, Guntuku S, Cui XS, et al. Chk1 is an essential kinase that is regulated by Atr and required for the G(2)/M DNA damage checkpoint. Genes Dev 2000;14:1448–1459.
21. Jackson JR, Gilmartin A, Imburgia C, Winkler JD, Marshall LA, Roshak A. An indolocarbazole inhibitor of human checkpoint kinase (Chk1) abrogates cell cycle arrest caused by DNA damage. Cancer Res 2000;60:566–572.
22. Hutchins JR, Dikovskaya D, Clarke PR. Regulation of Cdc2/cyclin B activation in Xenopus egg extracts via inhibitory phosphorylation of Cdc25C phosphatase by Ca(2+)/calmodulin-dependent protein [corrected] kinase II. Mol Biol Cell 2003;14:4003–4014.
23. Kawabe T. G2 checkpoint abrogators as anticancer drugs. Mol Cancer Ther 2004;3:513–519.
24. Siddiqui KM, Chopra DP. Primary and long term epithelial cell cultures from human fetal normal colonic mucosa. In Vitro 1984;20:859–868.
25. Lee WS, Chen RJ, Wang YJ, et al. In vitro and in vivo studies of the anticancer action of terbinafine in human cancer cell lines: G_0/G_1 p53-associated cell cycle arrest. Int J Cancer 2003;106:125–137.
26. Ho YS, Duh JS, Jeng JH, et al. Griseofulvin potentiates antitumorigenesis effects of nocodazole through induction of apoptosis and G2/M cell cycle arrest in human colorectal cancer cells. Int J Cancer 2001;91:393–401.
27. Wu CH, Jeng JH, Wang YJ, et al. Antitumor effects of miconazole on human colon carcinoma xenografts in nude mice through induction of apoptosis and G_0/G_1 cell cycle arrest. Toxicol Appl Pharmacol 2002;180:22–35.
28. Palermo C, Walworth NC. Assaying cell cycle checkpoints: Activity of the protein kinase Chk1. Methods Mol Biol 2005; 296:345–354.
29. Zhao B, Bower MJ, McDevitt PJ, et al. Structural basis for Chk1 inhibition by UCN-01. J Biol Chem 2002;277:46609–46615.
30. McGowan CH, Russell P. Human Wee1 kinase inhibits cell division by phosphorylating p34cdc2 exclusively on Tyr15. EMBO J 1993;12:75–85.
31. McGowan CH, Russell P. Cell cycle regulation of human WEE1. EMBO J 1995;14:2166–2175.
32. Yan Y, Mumby MC. Distinct roles for PP1 and PP2A in phosphorylation of the retinoblastoma protein. PP2a regulates the activities of G cyclin-dependent kinases. J Biol Chem 1999;274:31917–31924.
33. Ho YS, Wang YJ, Lin JK. Induction of p53 and p21/WAF1/CIP1 expression by nitric oxide and their association with apoptosis in human cancer cells. Mol Carcinog 1996;16: 20–31.
34. Ho YS, Ma HY, Chang HY, et al. Lipid peroxidation and cell death mechanisms in rats and human cells induced by chloral hydrate. Food Chem Toxicol 2003;41:621–629.
35. Lin SY, Chang YT, Liu JD, et al. Molecular mechanisms of apoptosis induced by magnolol in colon and liver cancer cells. Mol Carcinog 2001;32:73–83.
36. Maianski NA, Geissler J, Srinivasula SM, Alnemri ES, Roos D, Kuijpers TW. Functional characterization of mitochondria in neutrophils: A role restricted to apoptosis. Cell Death Differ 2004;11:143–153.
37. Liu JD, Wang YJ, Chen CH, et al. Molecular mechanisms of G_0/G_1 cell-cycle arrest and apoptosis induced by terfenadine in human cancer cells. Mol Carcinog 2003;37:39–50.
38. Wang YJ, Yu CF, Chen LC, et al. Ketoconazole potentiates terfenadine-induced apoptosis in human Hep G2 cells through inhibition of cytochrome p450 3A4 activity. J Cell Biochem 2002;87:147–159.
39. Grant JA, Danielson L, Rihoux JP, DeVos C. A double-blind, single-dose, crossover comparison of cetirizine, ebastine, epinastine, fexofenadine, terfenadine, and loratadine versus placebo: Suppression of histamine-induced wheal and flare response for 24 h in healthy male subjects. Allergy 1999;54: 700–707.
40. Nyberg KA, Michelson RJ, Putnam CW, Weinert TA. Toward maintaining the genome: DNA damage and replication checkpoints. Annu Rev Genet 2002;36:617–656.
41. Tseng CJ, Wang YJ, Liang YC, et al. Microtubule damaging agents induce apoptosis in HL 60 cells and G_2/M cell cycle arrest in HT 29 cells. Toxicology 2002;175:123–142.
42. Guo Z, Kumagai A, Wang SX, Dunphy WG. Requirement for Atr in phosphorylation of Chk1 and cell cycle regulation in response to DNA replication blocks and UV-damaged DNA in Xenopus egg extracts. Genes Dev 2000;14:2745–2756.
43. Sanchez Y, Wong C, Thoma RS, et al. Conservation of the Chk1 checkpoint pathway in mammals: Linkage of DNA damage to Cdk regulation through Cdc25. Science 1997; 277:1497–1501.
44. Furnari B, Rhind N, Russell P. Cdc25 mitotic inducer targeted by chk1 DNA damage checkpoint kinase. Science 1997;277: 1495–1497.
45. Matsuoka S, Huang M, Elledge SJ. Linkage of ATM to cell cycle regulation by the Chk2 protein kinase. Science 1998; 282:1893–1897.
46. Han EK, Butler C, Zhang H, et al. Chkl binds and phosphorylates BAD protein. Anticancer Res 2004;24:3907–3910.
47. Masters SC, Yang H, Datta SR, Greenberg ME, Fu H. 14-3-3 inhibits Bad-induced cell death through interaction with serine-136. Mol Pharmacol 2001;60:1325–1331.
48. Curman D, Cinel B, Williams DE, et al. Inhibition of the G2 DNA damage checkpoint and of protein kinases Chk1 and

Chk2 by the marine sponge alkaloid debromohymenialdisine. J Biol Chem 2001;276:17914–17919.
49. Sarkaria JN, Busby EC, Tibbetts RS, et al. Inhibition of ATM and ATR kinase activities by the radiosensitizing agent, caffeine. Cancer Res 1999;59:4375–4382.
50. Zhou BB, Chaturvedi P, Spring K, et al. Caffeine abolishes the mammalian G(2)/M DNA damage checkpoint by inhibiting ataxia-telangiectasia-mutated kinase activity. J Biol Chem 2000;275:10342–10348.
51. Blasina A, Price BD, Turenne GA, McGowan CH. Caffeine inhibits the checkpoint kinase ATM. Curr Biol 1999;9:1135–1138.
52. Wang YJ, Jeng JH, Chen RJ, et al. Ketoconazole potentiates the antitumor effects of nocodazole: In vivo therapy for human tumor xenografts in nude mice. Mol Carcinog 2002; 34:199–210.
53. Godlewski MM, Gajkowska B, Lamparska-Przybysz M, Motyl T. Colocalization of BAX with BID and VDAC-1 in nimesulide-induced apoptosis of human colon adenocarcinoma COLO 205 cells. Anticancer Drugs 2002;13:1017–1029.
54. Godlewski MM, Motyl MA, Gajkowska B, Wareski P, Koronkiewicz M, Motyl T. Subcellular redistribution of BAX during apoptosis induced by anticancer drugs. Anticancer Drugs 2001;12:607–617.
55. Hong SJ, Dawson TM, Dawson VL. Nuclear and mitochondrial conversations in cell death: PARP-1 and AIF signaling. Trends Pharmacol Sci 2004;25:259–264.
56. Qin H, Srinivasula SM, Wu G, Fernandes-Alnemri T, Alnemri ES, Shi Y. Structural basis of procaspase-9 recruitment by the apoptotic protease-activating factor 1. Nature 1999;399: 549–557.
57. Ho CC, Siu WY, Chow JP, et al. The relative contribution of CHK1 and CHK2 to Adriamycin-induced checkpoint. Exp Cell Res 2005;304:1–15.
58. Xiao Z, Xue J, Semizarov D, Sowin TJ, Rosenberg SH, Zhang H. Novel indication for cancer therapy: Chk1 inhibition sensitizes tumor cells to antimitotics. Int J Cancer 2005.
59. Powell SN, DeFrank JS, Connell P, et al. Differential sensitivity of p53(−) and p53(+) cells to caffeine-induced radiosensitization and override of G_2 delay. Cancer Res 1995; 55:1643–1648.
60. Russell KJ, Wiens LW, Demers GW, Galloway DA, Plon SE, Groudine M. Abrogation of the G_2 checkpoint results in differential radiosensitization of G_1 checkpoint-deficient and G_1 checkpoint-competent cells. Cancer Res 1995;55: 1639–1642.
61. Wang Y, Decker SJ, Sebolt-Leopold J. Knockdown of Chk1, Wee1 and Myt1 by RNA interference abrogates G2 checkpoint and induces apoptosis. Cancer Biol Ther 2004; 3:305–313.
62. Kumagai A, Guo Z, Emami KH, Wang SX, Dunphy WG. The Xenopus Chk1 protein kinase mediates a caffeine-sensitive pathway of checkpoint control in cell-free extracts. J Cell Biol 1998;142:1559–1569.
63. Luciani MG, Oehlmann M, Blow JJ. Characterization of a novel ATR-dependent, Chk1-independent, intra-S-phase checkpoint that suppresses initiation of replication in Xenopus. J Cell Sci 2004;117:6019–6030.
64. Bartkova J, Horejsi Z, Koed K, et al. DNA damage response as a candidate anti-cancer barrier in early human tumorigenesis. Nature 2005;434:864–870.
65. Tu LC, Matsui SI, Beerman TA. Hedamycin, a DNA alkylator, induces (gamma)H2AX and chromosome aberrations: Involvement of phosphatidylinositol 3-kinase-related kinases and DNA replication fork movement. Mol Cancer Ther 2005;4: 1175–1185.
66. Dhanalakshmi S, Agarwal C, Singh RP, Agarwal R. Silibinin up-regulates DNA-protein kinase-dependent p53 activation to enhance UVB-induced apoptosis in mouse epithelial JB6 cells. J Biol Chem 2005;280:20375–20383.
67. Manni I, Mazzaro G, Gurtner A, et al. NF-Y mediates the transcriptional inhibition of the cyclin B1, cyclin B2, and cdc25C promoters upon induced G_2 arrest. J Biol Chem 2001;276:5570–5576.
68. Yan Y, Spieker RS, Kim M, Stoeger SM, Cowan KH. BRCA1-mediated G_2/M cell cycle arrest requires ERK1/2 kinase activation. Oncogene 2005.
69. Yarden RI, Pardo-Reoyo S, Sgagias M, Cowan KH, Brody LC. BRCA1 regulates the G_2/M checkpoint by activating Chk1 kinase upon DNA damage. Nat Genet 2002;30:285–289.
70. Theron T, Bohm L. Cyclin B1 expression in response to abrogation of the radiation-induced G_2/M block in HeLa cells. Cell Prolif 1998;31:49–57.
71. Brown JW, Cappell S, Perez-Stable C, Fishman LM. Extracts from two marine sponges lower cyclin B1 levels, cause a G_2/M cell cycle block and trigger apoptosis in SW-13 human adrenal carcinoma cells. Toxicon 2004;43:841–846.
72. Scaife RM. G_2 cell cycle arrest, down-regulation of cyclin B, and induction of mitotic catastrophe by the flavoprotein inhibitor diphenyleneiodonium. Mol Cancer Ther 2004;3: 1229–1237.
73. Bulavin DV, Higashimoto Y, Demidenko ZN, et al. Dual phosphorylation controls Cdc25 phosphatases and mitotic entry. Nat Cell Biol 2003;5:545–551.
74. Smits VA, Medema RH. Checking out the G(2)/M transition. Biochim Biophys Acta 2001;1519:1–12.
75. Hsu SY, Kaipia A, Zhu L, Hsueh AJ. Interference of BAD (Bcl-xL/Bcl-2-associated death promoter)-induced apoptosis in mammalian cells by 14-3-3 isoforms and P11. Mol Endocrinol 1997;11:1858–1867.